Improvement of Thermal and Mechanical Properties of a Phenolic Resin Nanocomposite by *In Situ* Formation of Silsesquioxanes from a Molecular Precursor

Michael R. Schütz,[1] Katrin Sattler,[1] Stefan Deeken,[2] Otto Klein,[2] Volker Adasch,[2] Christian H. Liebscher,[3] Uwe Glatzel,[3] Jürgen Senker,[1] Josef Breu[1]

[1]*Lehrstuhl für Anorganische Chemie I, Universität Bayreuth, Bayreuth 95440, Germany*
[2]*Dronco AG, Wunsiedel 95632, Germany*
[3]*Lehrstuhl Metallische Werkstoffe, Universität Bayreuth, Bayreuth 95440, Germany*

Received 15 September 2009; accepted 27 December 2009
DOI 10.1002/app.32004
Published online 13 April 2010 in Wiley InterScience (www.interscience.wiley.com).

ABSTRACT: Silsesquioxanes are formed *in situ* during mixing and curing of a phenolic resin and a molecular silane precursor (3-(triethoxysilyl)-1-propaneamine) yielding a nanocomposite. As indicated by a higher onset temperature, a higher characteristic decomposition temperature, and a lower maximum heat flow, the thermal stability of the nanocomposite is significantly improved over the pristine resin. Moreover, the bending strength and the strain at break could also be enhanced by 36% and 51%, respectively. The nanocomposite was characterized by ^{29}Si solid-state NMR, STEM/EDS, TGA, DSC, and three point bending tests. The STEM/EDS measurements showed a homogenous distribution of silsesquioxanes in the phenolic resin. © 2010 Wiley Periodicals, Inc. J Appl Polym Sci 117: 2272–2277, 2010

Key words: nanocomposites; NMR; thermal properties; mechanical properties; POSS

INTRODUCTION

Organic–inorganic hybrid materials have been extensively studied over the last decades. Particularly, polymer nanocomposites have attracted large interest. Among other advantages, these composite materials offer enhanced mechanical and thermal properties.[1] The vast majority of publications focus on polyolefinic, polyamide matrices, and epoxy resins. Work on phenolic resins is scarce. These heat curing polymers are, however, widely used in a range of commercial applications as binder with good mechanical, electrical, and thermal properties.[2] Different nanoscopic fillers for phenolic resins like silica and clays have been studied to improve the physical properties of the composite materials.[3–7] One particularly interesting group of fillers applied, among others, to resole-type phenolic resins are silsesquioxanes. These are often used as nanoparticles in a defined geometry, so called polyhedral oligomeric silsesquioxanes (POSS).[8–12]

In brief, silsesquioxanes consist of a Si—O—Si network with one organic substituent attached to each silicon atom yielding a formula of $RSiO_{1.5}$.[13] The organic substituents allow adjusting the hydrophobicity and additionally may be utilized to link the filler covalently or by specific hydrogen bonding to the polymer matrix.

As the dimensions of the silsesquioxane particles are much smaller than those of typical clay or silica particles, the surface to volume ratio is much higher. Consequently, silsesquioxanes represent an attractive class of inorganic fillers to prepare nanocomposites.

Many silsesquioxane containing hybrid materials show improved thermal stability because char formation is promoted and diffusion of gases into the composite material is retarded.[14] Additionally, the mechanical properties of the nanocomposites are significantly improved by a more efficient energy dissipation via the Si—O—Si network during the fracture of the composite.[15]

We present the synthesis of a nanocomposite consisting of a resole-type phenolic resin matrix and a silsesquioxane. Applying a molecular silane precursor (3-(triethoxysilyl)-1-propaneamine, Fig. 1), the silsesquioxane was synthesized *in situ* in the phenolic resin. The composite was characterized by solid-state nuclear magnetic resonance (NMR) spectroscopy, by scanning transmission electron microscopy (STEM), and energy dispersive X-ray spectroscopy

Correspondence to: J. Breu (josef.breu@uni-bayreuth.de).
Contract grant sponsor: Federal state of Bavaria, Germany (Neue Werkstoffe – Unternehmen); contract grant number: NW-0608-0003.
Contract grant sponsor: Bavarian Elite Support Program.

© 2010 Wiley Periodicals, Inc.

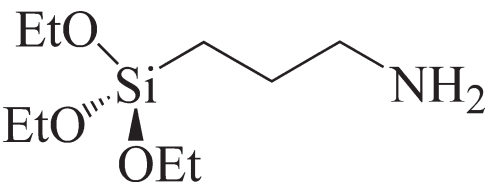

Figure 1 Molecular silane precursor 3-(triethoxysilyl)-1-propaneamine.

(EDS). Furthermore, the mechanical and thermal properties were examined by bending tests and thermogravimetric analysis/differential scanning calorimetry (TGA/DSC).

EXPERIMENTAL

Instrumentation and characterization

High resolution magic angle spinning solid-state ^{13}C and ^{29}Si NMR measurements were carried out at room temperature using a Bruker Avance II 300 MHz spectrometer (Rheinstetten, Germany) with resonance frequencies of 75.4 MHz and 59.6 MHz for ^{13}C and ^{29}Si, respectively. ^{13}C and ^{29}Si shifts were referenced relative to TMS. The samples were ground for 1 h in a ball mill, filled in 4-mm ZrO_2 rotors, mounted in a double resonance probe (Bruker), and rotated with spinning frequencies between 8 kHz and 13 kHz. A ramped cross-polarization sequence with contact times between 5 ms and 20 ms was used to excite both the ^{13}C and ^{29}Si nuclei via the proton bath. All 1D experiments were recorded using broadband proton decoupling via the SPINAL64 sequence.[16]

The electron micrographs and the EDS element maps were measured on a Zeiss (Oberkochen, Germany) Libra 200 FE transmission electron microscope operated at 200 kV. Measurements were performed using scanning transmission electron microscopy with a high angle annular dark field (HAADF) detector. Spot sizes between 12 and 15 nm were used for EDS analysis to ensure proper count rate statistics. Specimens were microtomed to 70–30 nm and placed on a copper grid.

A NETZSCH (Selb, Germany) STA 409 TGA/DSC apparatus was used to determine the thermal properties of the composite. The heating rate was 5 K min^{-1} and synthetic air or nitrogen was used as atmospheres. The sample mass was typically about 10 mg. The samples were ground and fractionated to <125 μm by sieving to achieve comparable specific surface areas.

The mechanical properties of the samples were measured by a Zwick (Ulm, Germany) Z020 universal three point bending tester at a load speed of 1 mm min^{-1} according to DIN EN ISO 178 (1 kN load cell). A minimum of eight specimens were tested for each sample.

MATERIALS AND METHODS

The resole-type phenolic resin was purchased from Fenolit d.d. (Slovenia). The silane 3-(triethoxysilyl)-1-propaneamine (Wacker Chemie AG, Germany) was applied as molecular precursor for synthesis of the silsesquioxane. All chemicals were used without further purification.

Preparation of the nanocomposite

The highly viscous phenolic resin and the 3-(triethoxysilyl)-1-propaneamine were mixed with a mechanical stirrer. The amount of silane was 10 wt % with respect to the phenolic resin. After thorough mixing with the silane, the resin was cured in a PTFE mould as described in the literature.[17]

RESULTS AND DISCUSSION

In situ synthesis of the silsesquioxanes

The phenolic resin used contains about 5 wt % of water. This low amount of water is fully sufficient to hydrolyze the ethoxy groups of the silane (estimated molar ratio: H_2O : Si-OEt = 18 : 10).[18] Hydrolysis is indicated by an increase of temperature of the resin during the addition of the silane. Clearly, reactive silanol groups are formed during the mixing of resin and silane. These reactive silanol groups then readily condense to oligomeric silsesquioxanes. This reaction changes the chemical environment of the silicon atoms resulting in a different isotropic shift in the ^{29}Si solid-state NMR.

Possible structures of the products with literature values of ^{29}Si NMR shifts are shown in Figure 2.[3,19] Because of the pronounced differences in the shifts, different hydrolysis and condensation grades can be followed by ^{29}Si solid-state NMR. The pristine, nonreacted silane shows a shift of about −42 ppm corresponding to a T^0 structure, which is in line with the literature values.[18]

The solid-state ^{29}Si NMR spectrum of the cured composite is shown in Figure 3. The spectrum was deconvoluted applying a Pseudo-Voigt peak function. The two signals at −58 ppm and −67 ppm correspond to T^2 and T^3 structures. Clearly, the monomeric precursor has undergone complete hydrolysis followed by the formation of highly condensed structures. The nearest hydrogen atoms around the silicon atoms are originating from the aminopropyl groups attached to each silicon atom. Therefore, as a first approximation, the two different condensed structures sense a similar hydrogen environment.

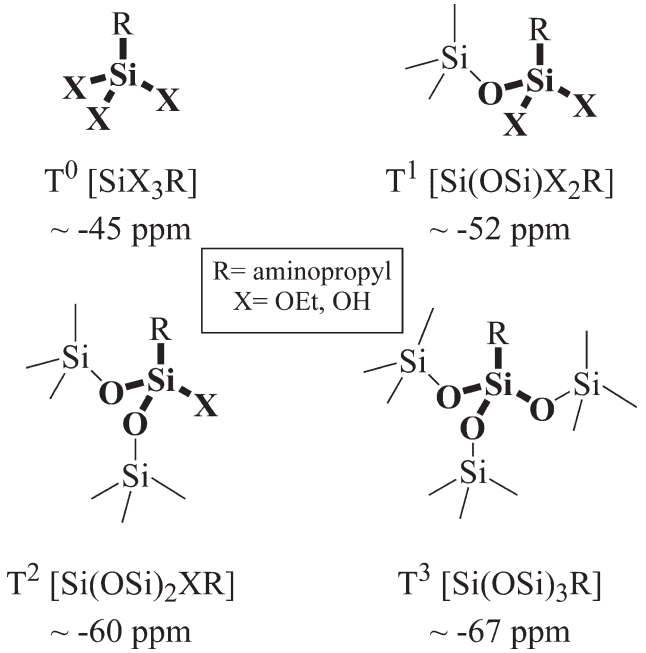

Figure 2 Possible structures of the silane and silsesquioxanes, respectively, with isotropic ^{29}Si shifts.

Consequently, although the spectrum is measured with cross-polarization, the intensities of the signals may be used to estimate the relative ratio of T^2 and T^3 structures. Integration of the peak areas showed that 92% of all silicon atoms are bonded to three neighboring silicon atoms by oxygen bridges (T^3 structures). The majority of the silane precursor thus formed silsesquioxanes during mixing and curing. Consequently, this network should be able to enhance the thermal and mechanical properties like POSS particles. At the rim of these silsesquioxanes,

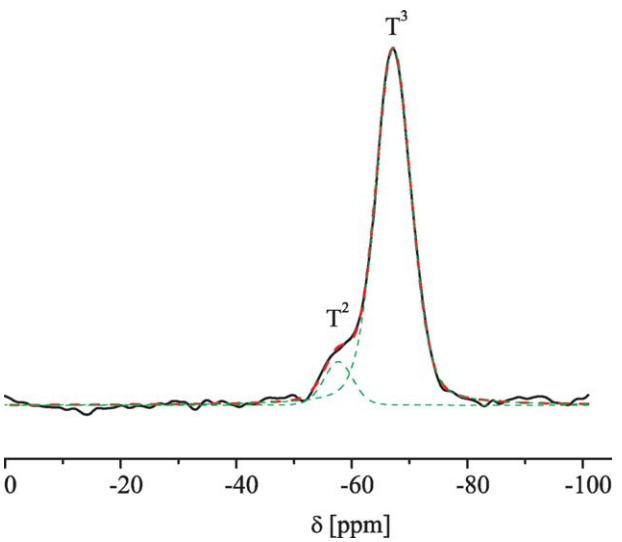

Figure 3 CP-MAS-^{29}Si spectrum of the synthesized nanocomposite with fitted isotropic shifts of T^2 and T^3 structures. [Color figure can be viewed in the online issue, which is available at www.interscience.wiley.com.]

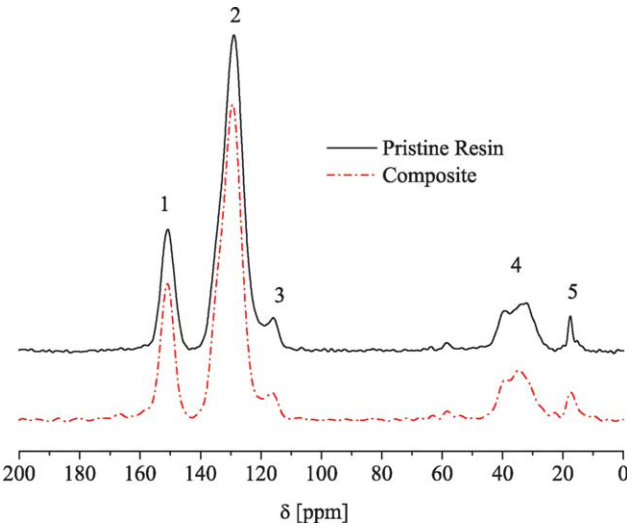

Figure 4 CP-MAS-^{13}C NMR spectra of the pristine resin and the composite. [Color figure can be viewed in the online issue, which is available at www.interscience.wiley.com.]

the degree of condensation must be lower and tangling groups are generated. Most likely, the remaining 8% of the silicon atoms may be attributed to these rims where the silicon atoms have two oxygen bridged silicon neighbors and one additional group (T^2 structures). This group may be a nonhydrolyzed ethoxy function, a hydrolyzed but noncondensed hydroxyl group, or a covalent silanol bond formed by reacting of Si—OH groups with functional groups of the resin during curing. For example, these groups in the resin could be the OH group of the phenol or a methoxy group of a condensation product (phenol and formaldehyde). Unfortunately, the resolution does not allow further deconvolution of the T^2 signal to distinguish these possibilities.

Therefore, ^{13}C solid-state NMR spectra were recorded for the pure resin and the *in situ* synthesized composite material (Fig. 4). Clearly, the degree of polymerization of both samples is quite high, as only a rather small peak is observed around 60 ppm, which is attributed to methylene ether bridges. These bridges are thermodynamically less stable and were mostly transformed to methylene bridges during curing. However, the observed peaks (Fig. 4, Peak 1–5) can all be attributed to the different carbon atoms in the completely cured resin.[20] Peak 1 derives from the ipso atoms of the phenolic ring, whereas Peaks 2 and 3 can be assigned to the other carbon atoms of the phenolic ring. In more detail, Peak 3 belongs to the nonsubstituted ortho or para positions. The range between 25 ppm and 45 ppm (Peak 4) derives from the methylene bridges between the phenolic rings. The peak at 17 ppm (Peak 5) is typical for methyl groups originating from decomposition of the resin during heating.[21] Since, the samples were prepared by grinding the

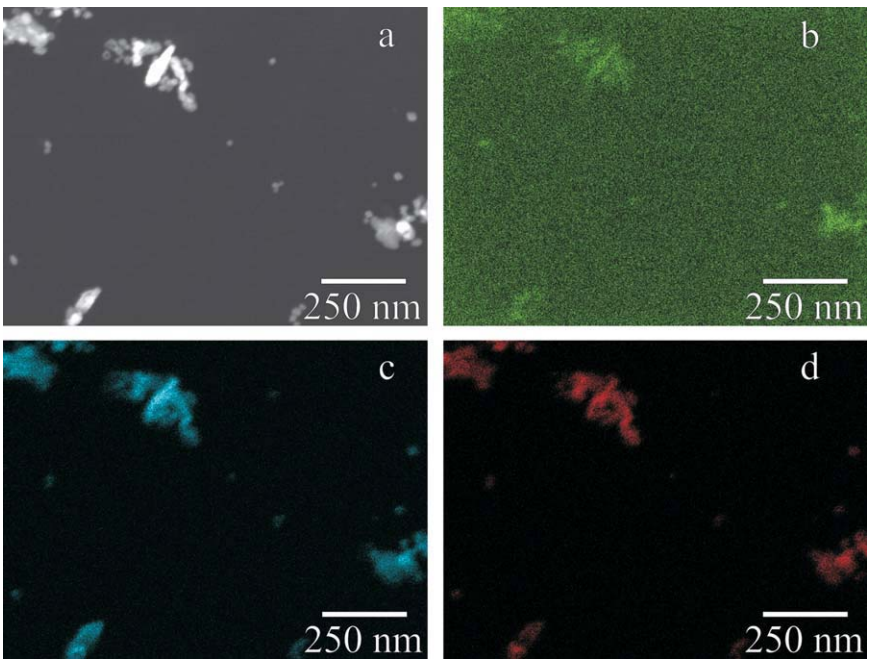

Figure 5 HAADF-STEM image of the composite with $BaSO_4$ originating from the catalyst (a), EDS element mappings of the same section for silicon (Si K line, b), barium (L line, c), and sulphur (K line, d). [Color figure can be viewed in the online issue, which is available at www.interscience.wiley.com.]

specimens in a ball mill also the energy introduced might have been sufficient to partially decompose the cured resin.

Please note that the moieties of the aminopropyl groups could not be assigned unequivocally in the ^{13}C solid-state NMR spectra. Therefore, it remains unclear whether the silsesquioxanes are not covalently linked to the resin matrix via Si—OH groups or whether these links are simply below the detection limit. Obviously, for the same reasons, nothing can be said about a possible covalent link of the filler to the polymer matrix via the NH_2– group of the aminopropyl groups present in both the T^2 and T^3 structures.

STEM/EDS measurements

The dispersion of the silsesquioxanes within the *in situ* synthesized nanocomposites was investigated by STEM and EDS measurements. Unfortunately, the element contrast of the TEM images recorded initially was hampered by considerable amounts of $BaSO_4$ present in the phenolic resin. Therefore, no particles or agglomerates of the silicon network could be detected. This $BaSO_4$ is formed by quenching the prepolymerization catalyst used for the phenol/formaldehyde condensation, $Ba(OH)_2$, with H_2SO_4. Consequently, the scanning TEM technique linked with EDS was used to improve the element contrast and investigate the distribution of the silsesquioxane in the nanocomposite (Fig. 5). All white spots visible in the STEM image [Fig. 5(a)]

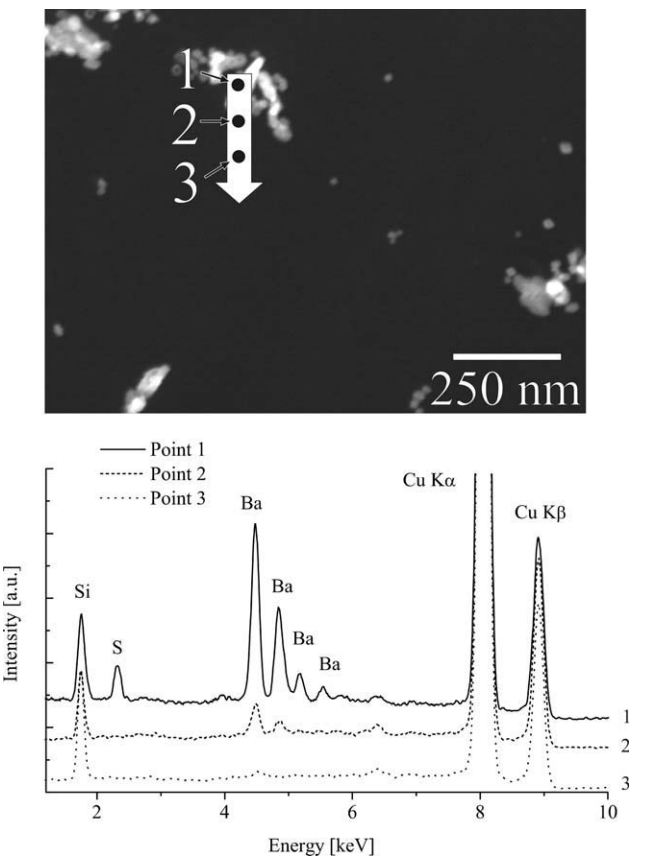

Figure 6 EDS spectra of the composite taken at selected points along the line indicated in the STEM image. EDS spectra were normalized to the intensity of the copper K_α line.

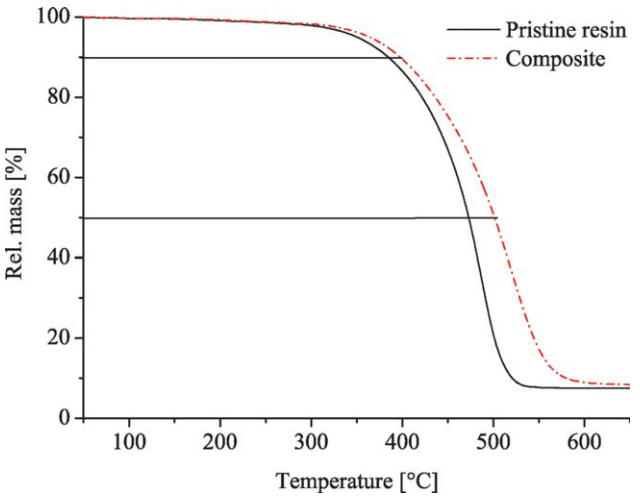

Figure 7 TGA curves of the pristine resin (line) and the composite (dotted) recorded in synthetic air. [Color figure can be viewed in the online issue, which is available at www.interscience.wiley.com.]

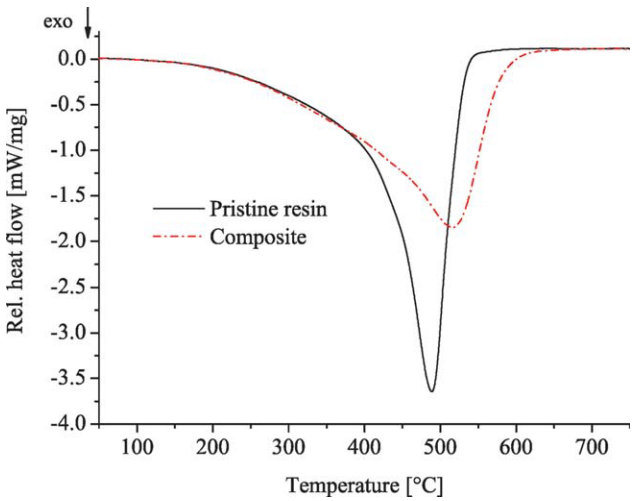

Figure 8 DSC curve of the pristine resin (line) and the composite (dotted) recorded in synthetic air. [Color figure can be viewed in the online issue, which is available at www.interscience.wiley.com.]

correspond to $BaSO_4$ particles and aggregates. EDS element mappings of Ba [Fig. 5(c)] and S [Fig. 5(d)] underline this assignment. The element mapping of Si shows a rather homogenous distribution of the silicon throughout the sample [Fig. 5(b)]. However, a slight accumulation of silicon at the surface of the $BaSO_4$ particles is noticeable.

A line scan was performed to quantify the homogenous distribution of silicon (Fig. 6). The EDS spectra of three points along this line scan have been normalized to the copper signal originating from the grid to allow comparison of the intensities. The silicon peak showed comparable intensity at all three chosen points (Point 1–3, Fig. 6) underlining the homogeneity of the dispersion of the silsesquioxanes within the *in situ* synthesized nanocomposites.

TGA/DSC analysis

The thermal stability of the composite was examined by TGA and DSC. Figure 7 shows the TGA curves of the pristine resin and the *in situ* synthesized nanocomposite measured in synthetic air. At low temperatures, a minute mass loss (<2%) is observed which can be attributed to release of surface water and pore water produced by further curing of the resin during TGA measurements. The onset of degradation temperature, as defined by the temperature of 10% mass loss ($T_{0.1}$), was determined to be 384°C for the pristine resin. The onset temperature of the nanocomposite is shifted by 13°C to 397°C. Furthermore, the decomposition of the pristine resin is faster than that of the composite material as indicated by the pace of mass loss. For instance, the temperature of 50% residual mass ($T_{0.5}$) increased for the composite as compared to the pure resin matrix by about 29°C (Table I).

Additional proof of the improved thermal oxidative stability of the nanocomposite is delivered by DSC (Fig. 8). The characteristic decomposition temperature (T_{max}), as defined by the maximum of the exothermal reaction, is significantly shifted by 28°C (488°C and 516°C for the pristine resin and the nanocomposite, respectively). In line with the TGA results, the nanocomposite decomposes more slowly

TABLE I
Thermal Properties of the Phenolic Resin and the Synthesized Nanocomposite

Sample	$T_{0.1}$ (°C)	$T_{0.5}$ (°C)	T_{max} (°C)
Pristine resin	384	472	488
Nanocomposite	397	501	516

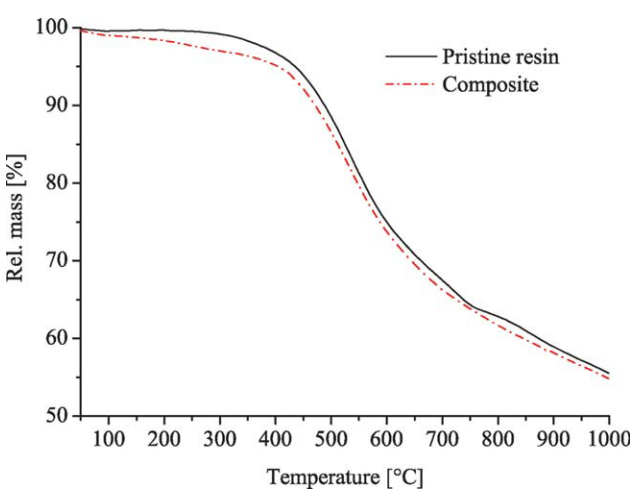

Figure 9 TGA curves of the pristine resin (line) and the composite (dotted) recorded in nitrogen. [Color figure can be viewed in the online issue, which is available at www.interscience.wiley.com.]

TABLE II
Mechanical Properties of the Pristine Resin and the Nanocomposite Determined by Three Point Bending Test

Sample	Young's modulus (MPa)	Bending strength (MPa)	Strain at beak (%)
Pristine resin	5600 ± 152	145 ± 15	2.5 ± 0.2
Nanocomposite	5400 ± 154	197 ± 23	3.8 ± 0.6

than the pristine resin. Additionally, the maximum relative heat flow of the nanocomposite is smaller than that of the pure resin, which suggests that the maximum heat release during the decomposition of the composite is lower as compared to the pure resin. Altogether, TGA and DSC measurements both suggest that the composite shows improved thermal oxidative stability. This may be explained by the formation of a protective layer of SiO_2 during pyrolysis of the silsesquioxanes at the surface of the nanocomposite.[22] This SiO_2 layer enhances char formation and this way might possibly retard the thermal oxidative degradation.[14] In comparison to those results, the TGA analysis in nitrogen showed no difference within experimental error between the pristine resin and the synthesized nanocomposite (Fig. 9). This suggests that the filler cannot change the decomposition mechanisms of the resin but retards the thermal oxidative degradation.

Three point bending tests

The mechanical properties of the *in situ* synthesized nanocomposites were investigated applying three point bending tests. Although Pittman et al.[10] reported higher storage moduli for POSS-modified phenolic resins, we find that within experimental error, the Young's modulus is the same for the pristine resin and the nanocomposite (Table II). Apparently, the *in situ* formed silsesquioxanes fail to enhance the stiffness of the composite. In contrast to the Young's modulus, the bending strength of the composite material is increased by 36% from 145 to 197 MPa as compared to the pristine resin. Additionally, the strain at break is improved by 52%. These enhancements may be explained by a more efficient energy dissipation during the fracture of the nanocomposite by the incorporation of the Si—O—Si network as suggested Musto et al.[15]

CONCLUSIONS

^{29}Si solid-state NMR proved that 3-(triethoxysilyl)-1-propaneamine is fully hydrolyzed upon mixing with a phenolic resin. Silsesquioxanes are formed by subsequent condensation and curing produces a nanocomposite *in situ*. STEM/EDS measurements showed a homogenous distribution of silicon in the phenolic resin, and no agglomerates or large particles were formed by condensation of the precursor.

Formation of a protective layer of SiO_2 during pyrolysis of the silsesquioxanes at the surface of the nanocomposite may be an important factor improving its thermal oxidative stability significantly. The onset of the decomposition and the characteristic decomposition temperature are higher for the nanocomposite as compared to the pristine resin (13°C and 28°C, respectively) and the oxidative decomposition of the matrix is retarded. Also the mechanical properties are improved by the *in situ* built silsesquioxane. Because of a more efficient energy dissipation of the nanocomposite through the Si—O—Si network, the bending strength and the strain at break could be enhanced by 36% and 51%, respectively.

The authors thank Dr. R. Giesa, department of Macromolecular Chemistry I, University of Bayreuth, for his assistance in building the test specimen. Furthermore, the authors are grateful to KEKUTEX Forschungs- und Innovationscenter e.V., Rehau, Germany for providing the three point bending test.

References

1. Krishnamoorti, R.; Vaia, R. A. Polymer Nanocomposites: Synthesis, Characterization and Modeling; American Chemical Society: Washington, DC, 2002.
2. Gardziella, A.; Pilato, L.; Knop, A. Phenolic Resins: Chemistry, Applications, Standardization, Safety, and Ecology; Springer: Berlin, 2000.
3. Chiang, C. L.; Ma, C. C. M.; Wu, D. L.; Kuan, H. C. J Polym Sci Polym Chem 2003, 41, 905.
4. Choi, M. H.; Chung, I. J.; Lee, J. D. Chem Mater 2000, 12, 2977.
5. Haraguchi, K.; Usami, Y.; Yamamura, K.; Matsumoto, S. Polymer 1998, 39, 6243.
6. Haraguchi, K.; Usami, Y.; Ono, Y. J Mater Sci 1998, 33, 3337.
7. Wu, Z. G.; Zhou, C. X.; Qi, R. R. Polym Compos 2002, 23, 634.
8. Huang, C. F.; Kuo, S. W.; Lin, F. J.; Huang, W. J.; Wang, C. F.; Chen, W. Y.; Chang, F. C. Macromolecules 2006, 39, 300.
9. Pittman, C. U.; Li, G. Z.; Ni, H. L. Macromol Symp 2003, 196, 301.
10. Pittman, C. U.; Li, G. Z.; Cho, H. S. J Inorg Organomet Polym Mater 2006, 16, 43.
11. Zhang, Y. D.; Lee, S. H.; Yoonessi, M.; Liang, K. W.; Pittman, C. U. Polymer 2006, 47, 2984.
12. Zhang, Y. D.; Lee, S. H.; Yoonessi, M.; Toghiani, H.; Pittman, C. U. J Inorg Organomet Polym Mater 2007, 17, 159.
13. Li, G. Z.; Wang, L. C.; Ni, H. L.; Pittman, C. U. J Inorg Organomet Polym 2001, 11, 123.
14. Lichtenhan, J. D. Comments Inorg Chem 1995, 17, 115.
15. Musto, P.; Ragosta, G.; Scarinzi, G.; Mascia, L. Polymer 2004, 45, 4265.
16. Fung, B. M.; Khitrin, A. K.; Ermolaev, K. J Magn Reson 2000, 142, 97.
17. Kaynak, C.; Cagatay, O. Polym Test 2006, 25, 296.
18. Beari, F.; Brand, M.; Jenkner, P.; Lehnert, R.; Metternich, H. J.; Monkiewicz, J.; Siesler, H. W. J Organomet Chem 2001, 625, 208.
19. Williams, E. A. The Chemistry of Organosilicon Compounds; Wiley: London, 1989.
20. Knop, A.; Pilato, L. A. Phenolic Resins—Chemistry, Applications and Performance; Springer-Verlag: Berlin, 1985.
21. Chen, Y. F.; Chen, Z. Q.; Xiao, S. Y.; Liu, H. B. Thermochim Acta 2008, 476, 39.
22. Liu, Y. R.; Huang, Y. D.; Liu, L. J Appl Polym Sci 2008, 110, 2989.